Highly Phosphorescent Bis-Cyclometalated Iridium Complexes: Synthesis, Photophysical Characterization, and Use in Organic Light Emitting Diodes

Sergey Lamansky,[†] Peter Djurovich,[†] Drew Murphy,[†] Feras Abdel-Razzaq,[†] Hae-Eun Lee,[†] Chihaya Adachi,[‡] Paul E. Burrows,[‡,§] Stephen R. Forrest,*[,‡] and Mark E. Thompson*[,†]

Contribution from the Department of Chemistry, University of Southern California, Los Angeles, California 90089, and Department of Electrical Engineering, Princeton University, Princeton, New Jersey 08544

Received October 16, 2000. Revised Manuscript Received February 23, 2001

Abstract: The synthesis and photophysical study of a family of cyclometalated iridium(III) complexes are reported. The iridium complexes have two cyclometalated (*C^N*) ligands and a single monoanionic, bidentate ancillary ligand (LX), i.e., $C\hat{}N_2$Ir(LX). The *C^N* ligands can be any of a wide variety of organometallic ligands. The LX ligands used for this study were all β-diketonates, with the major emphasis placed on acetylacetonate (acac) complexes. The majority of the $C\hat{}N_2$Ir(acac) complexes phosphoresce with high quantum efficiencies (solution quantum yields, 0.1−0.6), and microsecond lifetimes (e.g., 1−14 μs). The strongly allowed phosphorescence in these complexes is the result of significant spin−orbit coupling of the Ir center. The lowest energy (emissive) excited state in these $C\hat{}N_2$Ir(acac) complexes is a mixture of ^{3}MLCT and $^3(\pi-\pi^*)$ states. By choosing the appropriate *C^N* ligand, $C\hat{}N_2$Ir(acac) complexes can be prepared which emit in any color from green to red. Simple, systematic changes in the *C^N* ligands, which lead to bathochromic shifts of the free ligands, lead to similar bathochromic shifts in the Ir complexes of the same ligands, consistent with "$C\hat{}N_2$-Ir"-centered emission. Three of the $C\hat{}N_2$Ir(acac) complexes were used as dopants for organic light emitting diodes (OLEDs). The three Ir complexes, i.e., bis(2-phenylpyridinato-N,C$^{2'}$)iridium(acetylacetonate) [ppy_2Ir(acac)], bis(2-phenyl benzothiozolato-N,C$^{2'}$)iridium(acetylacetonate) [bt_2Ir(acac)], and bis(2-(2′-benzothienyl)-pyridinato-N,C$^{3'}$)iridium(acetylacetonate) [btp_2Ir(acac)], were doped into the emissive region of multilayer, vapor-deposited OLEDs. The ppy_2Ir(acac)-, bt_2Ir(acac)-, and btp_2Ir(acac)-based OLEDs give green, yellow, and red electroluminescence, respectively, with very similar current−voltage characteristics. The OLEDs give high external quantum efficiencies, ranging from 6 to 12.3%, with the ppy_2Ir(acac) giving the highest efficiency (12.3%, 38 lm/W, >50 Cd/A). The btp_2Ir(acac)-based device gives saturated red emission with a quantum efficiency of 6.5% and a luminance efficiency of 2.2 lm/W. These $C\hat{}N_2$Ir(acac)-doped OLEDs show some of the highest efficiencies reported for organic light emitting diodes. The high efficiencies result from efficient trapping and radiative relaxation of the singlet and triplet excitons formed in the electroluminescent process.

Introduction

The photophysics of octahedral $4d^6$ and $5d^6$ complexes has been studied extensively.[1] These complexes, particularly those prepared with Ru and Os, have been used in a variety of photonic applications, including photocatalysis and photoelectrochemistry.[2] These d^6 complexes are attractive in photochemical applications, because they generally have long-lived excited states and high luminescence efficiencies, increasing the likelihood of either energy or electron transfer occurring prior to radiative or nonradiative relaxation. Strong spin−orbit coupling of the 4d or 5d ion leads to efficient intersystem crossing of the singlet excited states to the triplet manifold.[3] The long lifetimes of these excited states are due to the triplet character of this state. Mixing of the singlet and triplet excited states, via spin−orbit coupling, removes the spin-forbidden nature of the radiative relaxation of the triplet state, leading to high phosphorescence efficiencies.

Researchers have directed their attention to the photochemistry and photophysics of Ru^{2+} and Os^{2+} complexes, with the majority of the effort being focused on metal−diimine complexes, such as the bipyridine and phenanthroline complexes.[4] More recently, researchers have investigated the photophysics

* To whom correspondence should be addressed: (S.R.F.) forrest@ee.princeton.edu. (M.E.T.) met@usc.edu.

† University of Southern California.

‡ Princeton University.

§ Current address: Pacific Northwest National Laboratory, K3-59 PO Box 999, Richland, WA 99352.

(1) (a) Balzani, V.; Scandola, F. *Supramolecular Photochemistry*; Ellis Horwood: Chichester, U.K., 1991. (b) Balzani, V.; Credi, A.; Scandola, F. In *Transition Metals in Supramolecular Chemistry*; Fabbrizzi, L., Poggi, A., Eds.; Kluwer: Dordrecht, The Netherlands, 1994; p1. (c) Lehn, J.-M. *Supramolecular Chemistry—Concepts and Properties*; VCH: Weinheim, Germany, 1995. (d) Bignozzi, C. A.; Schoonover, J. R.; Scandola, F. *Prog. Inorg. Chem.* **1997**, *44*, 1.

(2) (a) Kalyanasundaran, K. *Coord. Chem. Rev.* **1982**, *46*, 159−244. (b) Chin, K.-F.; Cheung, K.-K.; Yip, H.-K.; Mak, T. C. W.; Che, C. M. *J. Chem. Soc., Dalton Trans.* **1995,** *4*, 657−665. (c) Sonoyama, N.; Karasawa, O.; Kaizu, Y. *J. Chem. Soc., Faraday Trans.* **1995,** *91*, 437−443. (d) Tan-Sien-Hee, L.; Mesmaeker, A. K−D. *J. Chem. Soc., Dalton Trans.* **1994**, *24*, 3651−3658. (e) Kalyanasundaram, K.; Gratzel, M. *Coord. Chem. Rev.* **1998**, *177*, 347−414.

(3) (a) Baldo, M. A.; O'Brien, D. F.; You Y.; Shoustikov, A.; Sibley, S.; Thompson, M. E.; Forrest, S. R. *Nature* **1998**, *395*, 151−154. (b) Baldo, M A.; Lamansky, S.; Burrows, P. E.; Thompson, M. E.; Forrest, S. R. *Appl. Phys. Lett.* **1999**, 75, 4−6. (c) Thompson, M. E.; Burrows, P. E.; Forrest, S. R. *Cur. Opinion Solid State Mater. Sci.* **1999**, *4*, 369.

10.1021/ja003693s CCC: $20.00
Published on Web 04/13/2001

of isoelectronic Rh^{3+} and Ir^{3+} complexes, with both diimine and cyclometalated ligands, such as 2-phenylpyidinato-C^2,N (*ppy*).[5] The cyclometalated ligands are formally monoanionic and can thus be used to prepare neutral tris-ligand complexes, which are isoelectronic with the cationic trisdiimine complexes of Ru and Os, e.g., *fac*-M(*ppy*)$_3$,[6] *fac*-M(2-(α-thiopheneyl)-pyridine)$_3$ (*fac* = facial).[7] The d^6 Ir complexes show intense phosphorescence at room temperature, while the Rh complexes give measurable emission only at low temperatures, consistent with stronger spin−orbit coupling of Ir relative to Rh. The electronic transitions responsible for luminescence in these complexes have been assigned to a mixture of metal-to-ligand charge-transfer (MLCT) and $^3(\pi-\pi^*)$ ligand states.[8] We have recently found that highly emissive Ir complexes can be formed with two cyclometalated ligands (abbreviated hereafter as *C^N*) and a single monoanionic, bidentate ancillary ligand (LX).[9] The emission colors from these complexes are strongly dependent on the choice of cyclometalating ligand, ranging from green to red, with room-temperature lifetimes from 1 to 14 μs. The photophysical properties of these *C^N*$_2$Ir(LX) complexes are similar to those observed for the tris-cyclometalated complexes, and will be discussed below.

Heavy metal complexes, particularly those containing Pt and Ir, can serve as efficient phosphors in organic light emitting devices.[10] In these devices, holes and electrons are injected into opposite surfaces of a planar multilayer organic thin film. The holes and electrons migrate through the thin film, to a material interface, where they recombine to form radiative excited states, or excitons. This electrically generated exciton can be either a singlet or a triplet. Both theoretical predictions and experimental measurements give a singlet/triplet ratio for these excitons of 1 to 3.[11] Fluorescent materials typically used to fabricate organic light emitting diodes (OLEDs) do not give detectable triplet emission (i.e., phosphorescence), nor is there evidence for significant intersystem crossing between the triplet and singlet manifolds at room temperature. The singlet/triplet ratio thus implies a limitation of 25% for the internal quantum efficiency for OLEDs based on fluorescence. By doping OLEDs with heavy metal phosphors, we have shown that the singlet−triplet limitation can be eliminated.[10] The excited states generated by electron−hole recombination are trapped at the phosphor, where strong spin−orbit coupling leads to singlet−triplet state mixing and, hence, efficient phosphorescent emission at room temperature. Both singlet and triplet excited states can be trapped at the phosphor. OLEDs prepared with these heavy metal complexes are the most efficient OLEDs reported to date, with internal quantum efficiencies exceeding 75% (photons/electrons) (>15% external efficiency).[12] Furthermore, OLEDs have been prepared with *C^N*$_2$Ir(LX) phosphor dopants, giving efficient green, yellow, or red emission. The external quantum efficiencies for these devices vary from 5% to nearly 20%. In this work, we explore the photophysical and electroluminescent properties of a series of Ir complexes used as efficient phosphorescent dopants in OLEDs. We demonstrate that, by optimizing the molecular structure of *C^N*$_2$Ir(LX) dopants and the energy-transfer process, exceedingly high external and power efficiencies can be obtained in the green to red spectral region.

Experimental Section

Synthesis. All synthetic procedures involving $IrCl_3 \cdot H_2O$ and other Ir(III) species were carried out in inert gas atmosphere despite the air stability of the compounds, the main concern being the oxidative stability of intermediate complexes at the high temperatures used in the reactions. NMR spectra were recorded on Bruker AMX 360- or 500-MHz instruments. High-resolution mass spectrometry was carried out by the mass specroscopy facility at the Frick Chemistry Laboratory, Princeton University. Elemental analyses (C, H, N) were carried out by standard combustion analysis by the Microanalysis Laboratory at the University of Illinois, Urbana−Champagne.

Cyclometalated Ir(III) μ-chloro-bridged dimers of a general formula *C^N*$_2$Ir(μ-Cl)$_2$Ir*C^N*$_2$ were synthesized according to the Nonoyama route, by refluxing $IrCl_3 \cdot nH_2O$ (Next Chimica) with 2−2.5 equiv of cyclometalating ligand in a 3:1 mixture of 2-ethoxyethanol (Aldrich Sigma) and water.[13]

C^N$_2$Ir(acac), *C^N* = *ppy*, *tpy*, *bzq*, *bt*, α*bsn*, and *pq* were prepared as described previously.[9]

Synthesis of (*C^N*)$_2$Ir(acac) Complexes. General Procedure. The chloro-bridged dimer complex (0.08 mmol), 0.2 mmol of acetyl acetone, and 85−90 mg of sodium carbonate were refluxed in an inert atmosphere in 2-ethoxyethanol for 12−15 h. After cooling to room temperature, a colored precipitate was filtered off and washed with water, hexane, and ether. The crude product was flash chromatographed on a silica column with dichloromethane mobile phase to yield ∼75−90% of the pure *C^N*$_2$Ir(acac), after solvent evaporation and drying.

thp$_2$Ir(acac): Iridium(III) bis(2-(2′-thienyl)pyridinato-N,C$^{3'}$) (acetyl acetonate) (yield 83%). ^{1}H NMR (360 MHz, acetone-d_6): δ, ppm 8.41 (d, 2H, *J* 5.8 Hz), 7.79 (td, 2H, *J* 7.9, 1.6 Hz), 7.56 (d, 2H, *J* 7.9 Hz), 7.22 (d, 2H, *J* 4.7 Hz), 7.11 (td, 2H, *J* 6.3, 1.6 Hz), 6.09 (d, 2H, *J* 4.7 Hz), 5.29 (s, 1H), 1.72 (s, 6H). Anal. Found C 45.33, H 3.00, N 4.81. Calcd C 45.16, H 3.13, N 4.58.

btp$_2$Ir(acac): Iridium(III) bis(2-(2′-benzothienyl)pyridinato-N,C$^{3'}$) (acetylacetonate) (yield 72%). ^{1}H NMR (360 MHz, acdtone-d_6): δ, ppm 8.39 (d, 2H, *J* 5.9 Hz), 7.80 (t, 2H, *J* 7.9 Hz), 7.77 (d, 2H, *J* 8.0 Hz), 7.68 (d, 2H, J 8.0 Hz), 7.25 (t, 2H, J 7.0 Hz), 7.10 (t, 2H, J 7.1 Hz), 6.82 (t, 2H, J 8.0 Hz), 6.40 (d, 2H, *J* 7.3 Hz), 5.70 (s, 1H), 1.90 (s, 6H). Anal. Found C 52.51, H 3.29, N 4.01. Calcd C 52.30, H 3.26, N 3.94.

dpo$_2$Ir(acac): Iridium(III) bis(2,4-diphenyloxazolato-1,3-N,C$^{2'}$) (acetyl acetonate) (yield 93%).^{1}H NMR (360 MHz, $CDCl_3$): δ, ppm 7.79 (d, 4H, *J* 7.4 Hz), 7.53 (d, 2H, *J* 7.9 Hz), 7.49 (m, 6H), 7.45 (s, 2H), 7.40 (t, 2H, *J* 7.4 Hz), 6.84 (t, 2H, *J* 7.4 Hz), 6.76 (t, 2H, *J* 7.4 Hz), 6.62 (d, 2H, *J* 7.9 Hz), 5.25 (s, 1H), 1.86 (s, 6H). Anal. Found C 56.35, H 3.67, N 3.89. Calcd C 57.44, H 3.72, N. 3.83.

C6$_2$Ir(acac): Iridium(III) bis(3-(2-benzothiazolyl)-7-(diethylamino)-2*H*-1-benzopyran-2-onato-N′,C^4) (acetyl acetonate) (yield 59%). ^{1}H

(4) (a) Anderson, P. A.; Anderson, R. F.; Furue, M.; Junk, P. C.; Keene, F. R.; Patterson, B. T.; Yeomans, B. D. *Inorg. Chem.* **2000**, *39*, 2721−2728. (b) Li, C.; Hoffman, M. Z. *Inorg. Chem.* **1998**, *37*, 830−832. (c) Berg-Brennan, C.; Subramanian, P.; Absi, M.; Stern, C.; Hupp, J. T. *Inorg. Chem.* **1996**, *35*, 3719−3722. (d) Kawanishi, Y.; Kitamura, N.; Tazuke, S. *Inorg. Chem.* **1989**, *28*, 2968−2975.

(5) (a) Balzani, V.; Juris, A.; Venturi, M.; Campagna, S.; Serroni, S. *Chem. Rev.* **1996**, *96*, 759−834. (b) Shaw, J. R.; Sadler, G. S.; Wacholtz, W. F.; Ryu, C. K.; Schmehl, R. H. *New J. Chem.* **1996**, *20*, 749.

(6) (a) Garces, F. O.; King, K. A.; Watts, R. J. *Inorg. Chem.* **1988**, *27*, 3464−3471. (b) Dedian, K.; Djurovich, P. I.; Garces, F. O.; Carlson, G.; Watts, R. J. *Inorg. Chem.* **1991**, *30*, 1685−1687. (c) Schmid, B.; Garces, F. O.; Watts, R. J. *Inorg. Chem.* **1994**, *33*, 9−14. (d) King, K. A.; Spellane, P. J.; Watts, R. J. *J. Am. Chem. Soc.* **1985**, *107*, 1432−1433.

(7) Colombo, M. G.; Brunold, T. C.; Riedener, T.; Güdel, H. U.; Förtsch, M.; Bürgi, H.-B. *Inorg. Chem.* **1994**, *33*, 545−550.

(8) (a) Wilde, A. P.; King, K. A.; Watts, R. J. *J. Phys. Chem.* **1991**, *95*, 629−634. (b) Sprouse, S.; King, K. A.; Spellane, P. J.; Watts, R. J. *J. Am. Chem. Soc.* **1984**, *106*, 6647−6653. (c) Crosby, G. A. *J. Chim. Phys.* **1967**, *64*, 160. (d) Columbo, M. C.; Hauser, A.; Güdel, H. U. *Top. Curr. Chem.* **1994**, *171*, 143.

(9) Lamansky, S.; Djurovich, P.; Murphy, D.; Abdel-Razaq, F.; Kwong, R.; Tsyba, I.; Bortz, M.; Mui, B.; Bau, R.; Thompson, M. E. *Inorg. Chem.* **2001**, *40*, 1704−1711.

(10) (a) Baldo, M. A.; O'Brien, D. F.; You, Y.; Shoustikov, A.; Sibley, S.; Thompson, M. E.; Forrest, S. R. *Nature* 1998, *395*, 151−154. (b) Baldo, M A.; Lamansky, S.; Burrows, P. E.; Thompson, M. E.; Forrest, S. R. *Appl. Phys. Lett.* 1999, 75, 4−6. (c) Thompson, M. E.; Burrows, P. E.; Forrest, S. R. *Curr. Opin. Solid State Mater. Sci.* 1999, *4*, 369.

(11) Baldo, M. A.; O'Brien, D. F.; Thompson, M. E.; Forrest, S. R. *Phys. Rev. B* **1999**, *60*, 14422.

(12) Adachi, C.; Baldo, M. A.; Forrest, S. R.; Thompson, M. E. *Appl. Phys. Lett.* **2000**, *78*, 1704.

(13) Nonoyama, M. *Bull. Chem. Soc. Jpn.* **1974**, *47*, 767−768.

Table 1. Photophysical Data for $C^{\wedge}N_2$Ir(acac) Complexes[a]

$C^{\wedge}N$ ligand	absorbance λ (log ϵ)	emission λ_{max} (nm)	lifetime (μs) 298 K	quantum efficiency
bo	262 (4.7), 269 (4.6), 298 (4.6), 310 (4.5), 343 (4.0), 383 (3.8), 425 (3.7), 462 (3.6), 510 (2.6)	525	1.1	0.25
bon	266 (4.8), 298 (4.7), 326 (4.6), 360 (4.4), 410 (4.1), 458 (4.0), 491 (4.0)	586	1.3	0.11
bzq[9]	260 (4.6), 360 (3.9), 470 (3.3), 500 (3.2)	548	4.5	0.27
α-*bsn*	274 (4.7), 300 (4.6), 345 (4.5), 427 (4.0), 476 (4.0), 506 (3.9)	606	1.8	0.22
β-bsn	328 (4.7), 348 (4.6), 420 (3.8), 496 (3.5)	594	2.2	0.16
btth	286 (4.4), 327 (4.4), 405 (4.0), 437 (4.0), 478 (3.9)	593	3.6	0.21
bt[9]	269 (4.6), 313 (4.4), 327 (4.5), 408 (3.8), 447 (3.8), 493 (3.4), 540 (3.0)	557	1.8	0.26
btp	286 (4.5), 340 (4.1), 355 (3.9), 495 (3.7)	612	5.8	0.21
C6	444 (4.8), 472 (4.8)	585	14	0.6
op	258 (4.4), 294 (4.2), 336 (4.1), 372 (3.8), 456 (3.5)	520	2.3	0.14
dpo	297 (4.8), 369 (4.0), 420 (3.9), 443 (3.9)	550	3.0	0.1
ppy[9]	260 (4.5), 345 (3.8), 412 (3.4), 460 (3.3), 497 (3.0)	516	1.6	0.34
pq[9]	268 (5.0), 349 (4.4), 433 (3.9), 467 (3.9), 553 (3.6)	597	2	0.1
thp	302 (4.4), 336 (4.1), 387 (3.8), 453 (3.5)	562	5.3	0.12
tpy[9]	270 (4.5), 370 (3.7), 410 (3.5), 460 (3.4), 495 (3.0)	512	3.1	0.31

[a] All of the data were collected for 2-methyltetrahydrofuran solutions.

NMR (360 MHz, $CDCl_3$): δ, ppm 7.86 (d, 2H, *J* 8.0 Hz), 7.58 (d, 2H, *J* 8.0 Hz), 7.29 (t, 2H, *J* 8.0 Hz), 7.21 (t, 2H, *J* 7.4 Hz), 6.29 (s, 2H), 6.05 (d, 2H, *J* 9.7 Hz), 5.83 (d, 2H, *J* 9.1 Hz), 5.27 (s, 1H), 3.20 (m, 8H), 1.68 (s, 6H), 1.03 (t, 12H, *J* 7.4 Hz). Anal. Found C 52.45, H 4.33, N 5.33. Calcd C 54.58, H 4.17, N 5.66.

bon$_2$Ir(acac): Iridium(III) bis(2-(1-naphthyl)benzooxazolato-N,C$^{2'}$) (acetyl acetonate) (yield 70%). ^{1}H NMR (360 MHz, $CDCl_3$): δ, ppm 1.82 (s,6 H), 5.24 (s, 1H), 6.70 (d, 2H, *J* 8.5 Hz), 7.07 (d, 2H, *J* 8.2 Hz),7.28 (t, 2H, *J* 7.5 Hz), 7.41(t, 2H, *J* 7.5 Hz), 7.47 (d, 2H, *J* 8.2 Hz), 7.55 (m, 6H), 7.80 (d, 2H, *J* 7.50 Hz), 8.89 (d, 2H, *J* 8.5 Hz). High-resolution MS: calculated M^+ 780.1600; observed M^+ 780.1592.

βbsn$_2$Ir(acac): Iridium(III) bis(2-(2-naphthyl)benzothiazolato-N,C$^{2'}$) (acetyl acetonate). (yield 70%). ^{1}H NMR (360 MHz, CD_2Cl_2): δ, ppm 8.25 (s, 2 H), 8.16 (d, 2 H, *J* 8 Hz), 8.05 (d, 2 H, *J* 8 Hz), 7.71 (t, 2 H, *J* 4.5 Hz), 7.52 (m, 4 H), 7.18 (m, 6 H), 6.74 (s, 2 H), 5.24 (s, 1 H), 1.79 (s, 6 H). Anal. Found C 56.68, H 3.22, N 3.59. Calcd C 56.56, H 3.51, N 3.03.

op$_2$Ir(acac): Iridium(III) bis(2-phenyl oxazolinato-N,C$^{2'}$(acetyl acetonate) (yield 70%). ^{1}H NMR (360 MHz, CD_2Cl_2): δ, ppm 7.26 (d, 2H, *J* 7.8 Hz), 6.86 (m, 4 H), 6.8 (t, 2H, *J* 6.8 Hz), 5.22 (s, 1 H), 4.98 (dd, 2H, *J* 8.6, 8.3 Hz), 4.87 (dd, 2H, *J* 8.6, 8.3 Hz), 4.04 (dd, 2H, *J* 12.7, 7.7 Hz), 3.82 (dd, 2H, *J* 12.7, 7.7 Hz), 1.80 (s, 6H). High-resolution MS: calculated M^+ 584.1287; observed M^+ 584.1295.

Optical Measurements. Absorption spectra were recorded on AVIV model 14DS UV−visible−IR spectrophotometer (re-engineered Cary 14) and corrected for background due to solvent absorption. Emission spectra were recorded on PTI QuantaMaster model C-60SE spectrofluorometer with 928 PMT detector and corrected for detector sensitivity inhomogeneity. Emission quantum yields were determined using *fac*-Ir(ppy)$_3$ as a reference.[14] Emission lifetimes were obtained by exponential fit of emission decay[15] curves recorded on a PTI TimeMaster model C-60SE spectrofluorometer.

OLED Fabrication and Testing. The OLED structure employed in this study is shown in the inset of Figure 6. Organic layers were fabricated by high-vacuum (10^{-6} Torr) thermal evaporation onto a glass substrate precoated with an indium−tin−oxide (ITO) layer with a sheet resistance of 20 Ω/□. Prior to use, the ITO surface was ultrasonicated in a detergent solution followed by a deionized water rinse, dipped into acetone, trichloroethylene, and 2-propanol, and then degreased in 2-propanol vapor. After degreasing, the substrate was oxidized and cleaned in a UV-ozone chamber before it was loaded into an evaporator. A 50-nm-thick film of 4,4′-bis[*N*-(naphthyl-*N*-phenylamino)biphenyl (α-NPD) served as the hole transport layer (HTL). The light emitting layer was prepared by coevaporating a 4,4′-*N*,*N*′-dicarbazolebiphenyl (CBP) host and a phosphorescent dopant, with both deposition rates being controlled with two independent quartz crystal oscillators. *ppy*$_2$Ir(acac), *bt*$_2$Ir(acac), and *btp*$_2$Ir(acac) with a dopant concentration of ∼7% were utilized to promote short-range Dexter transfer of the triplet excitons without concentration quenching.[1] Next, a 10-nm-thick 2,9-dimethyl-4,7-diphenyl-1,10-phenanthroline (BCP) as a hole and exciton blocking layer (HBL) and 40-nm-thick tris(8-hydroxyquinoline)-aluminum (Alq$_3$) as an electron transport layer were deposited on the emitter layer. Finally, a shadow mask with 1-mm-diameter openings was used to define the cathode consisting of a 100-nm-thick Mg−Ag layer, with a 20-nm-thick Ag cap. Current density−voltage−luminance (J−V−L) measurements were obtained using a semiconductor parameter analyzer and a calibrated silicon photodiode.

(14) King, K. A.; Spellane, P. J.; Watts, R. J. *J. Am. Chem. Soc.* **1985**, *107*, 1432−1433.

(15) O'Connor, D. V.; Phillips, D. *Time-Correlated Single Photon Counting*; Academic Press: London, 1984; p 287.

Results and Discussion

Synthesis and Characterization of $C^{\wedge}N_2$Ir(LX) Complexes. $C^{\wedge}N_2$Ir(LX) complexes have been prepared, with several different $C^{\wedge}N$ and LX ligands, Figure 1 and Table 1. The synthetic procedure used to prepare these complexes involves two steps.[9] In the first step, $IrCl_3 \cdot nH_2O$ is reacted with an excess of the desired $C^{\wedge}N$ ligand to give a chloride-bridged dimer, i.e., $C^{\wedge}N_2$Ir(μ-Cl)$_2$Ir$C^{\wedge}N_2$, eq 1. The NMR spectra of these complexes

$$2IrCl_3 \cdot nH_2O + 2C^{\wedge}NH \rightarrow C^{\wedge}N_2Ir(\mu\text{-}Cl)_2IrC^{\wedge}N_2 + 2HCl + 2Cl \quad (1)$$

$$C^{\wedge}N_2Ir(\mu\text{-}Cl)_2IrC^{\wedge}N_2 + 2LXH \rightarrow 2C^{\wedge}N_2Ir(LX) + 2HCl \quad (2)$$

are consistent with the heterocyclic rings of the $C^{\wedge}N$ ligands being in a trans disposition, as shown in Figure 1b. The chloride-bridged dimers can be readily converted to emissive, monomeric complexes by replacing the bridging chlorides with bidentate, monoanionic β-diketonate ligands (LX), eq 2. These reactions give $C^{\wedge}N_2$Ir(LX) with a yield of typically >80%.

X-ray crystallographic studies have been carried out for two $C^{\wedge}N_2$Ir(LX) complexes, i.e., (*ppy*)$_2$Ir(acac) and (*tpy*)$_2$Ir(acac) (acac = acetylacetonate).[9] The Ir in both of these $C^{\wedge}N_2$Ir(acac) complexes is octahedrally coordinated by the three chelating ligands, with the pyridyl groups in a trans disposition, as shown schematically in Figure 1b. The coordination geometries of the "$C^{\wedge}N_2$Ir" fragment in both the *tpy* and *ppy* iridium acac complexes are the same as that reported for the chloride-bridged

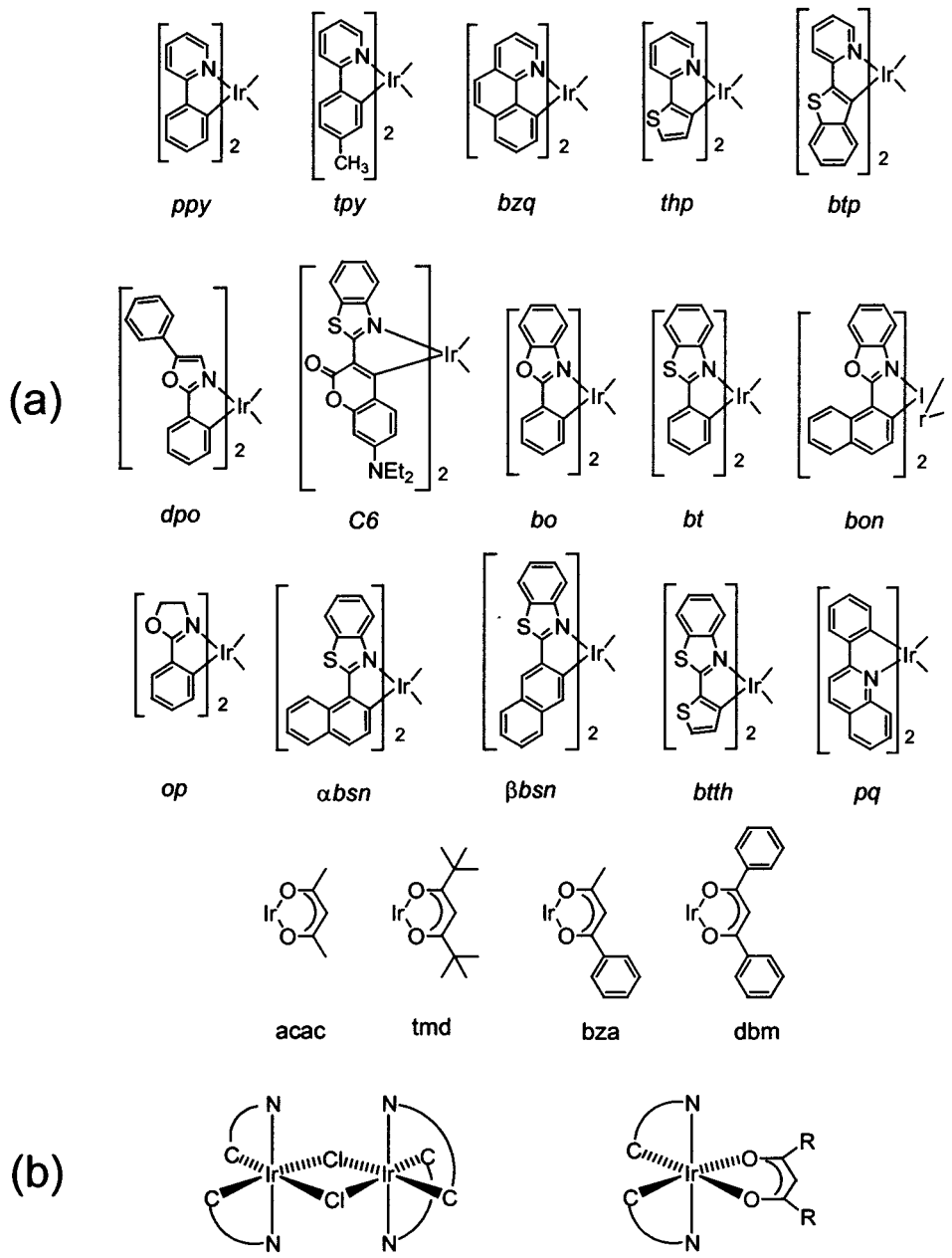

Figure 1. Cyclometalating (*C^N*) and ancillary (LX) ligands used to prepare $C\text{^}N_2$Ir(LX) complexes, (a). The abbreviations used throughout the paper for each ligand are listed below the "$C\text{^}N_2$Ir" or "Ir(LX)" fragment. The coordination geometries of the chloride-bridged dimer and $C\text{^}N_2$-Ir(LX) complexes are shown in (b).

dimers and $C\text{^}N_2$Ir(bpy)$^+$ complexes of the same *C^N* ligands.[16] The $C\text{^}N_2$Ir(LX) complexes are stable in air and can be sublimed in a vacuum without decomposition.

Photophysical Properties of $C\text{^}N_2$Ir(LX) Complexes. In order for the $C\text{^}N_2$Ir(LX) complexes to be useful as phosphors in organic light emitting diodes, strong spin−orbit coupling must be present to efficiently mix the singlet and triplet excited states. Clear evidence for significant mixing of the singlet and triplet excited states is seen in both the absorption and emission spectra of these complexes. All of the $C\text{^}N_2$Ir(LX) complexes show intense absorption from *C^N* ligand $\pi-\pi^*$ and MLCT transitions. The absorption spectra for the *ppy*, *bzq*, *thp*, and *btp* complexes are shown in Figure 2. The extinction coefficients for these bands are in the ranges expected for $\pi-\pi^*$ ligand-centered and MLCT bands, about 10 000−35 000 and 2000−6000 M^{-1} cm^{-1}, respectively. The $\pi-\pi^*$ absorption bands for these complexes fall in the ultraviolet and closely resemble the spectra of the free *C^N* ligands. Both ^{1}MLCT and ^{3}MLCT bands are typically observed for these complexes. The high degree of spin−orbit coupling is evident in comparing the oscillator strengths for the two MLCT bands. For example, the singlet and triplet MLCT bands for ppy_2Ir(acac) fall at 410 and 460 nm, respectively (see Figure 2 and Table 1), with less than a factor of 2 difference in their extinction coefficients. Strong spin−orbit coupling on Ir gives the formally spin-forbidden ^{3}MLCT an intensity comparable to the allowed ^{1}MLCT. The energies of these singlet and triplet MLCT absorptions are very similar to those reported for ppy_2Ir(bpy)$^+$,[17] ppy_2Ir(H$_2$O)$_2^+$,[18]

(16) Carlson, G. A.; Djurovich, P. I.; Watts, R. J. *Inorg. Chem.* **1993**, *32*, 4483−4484.

(17) (a) Ohsawa, Y.; Sprouse, S.; King, K. A.; DeArmond, M. K.; Hanck, K. W.; Watts, R. J. *J. Phys. Chem.* **1987**, *91*, 1047−1058. (b) Colombo, M. G.; Hauser, A.; Gudel, H. U. *Inorg. Chem.* **1993**, *32*, 3088−3092.

(18) Schmid, B.; Garces, F. O.; Watts, R. J. *Inorg. Chem.* **1994**, *33*, 9−14.

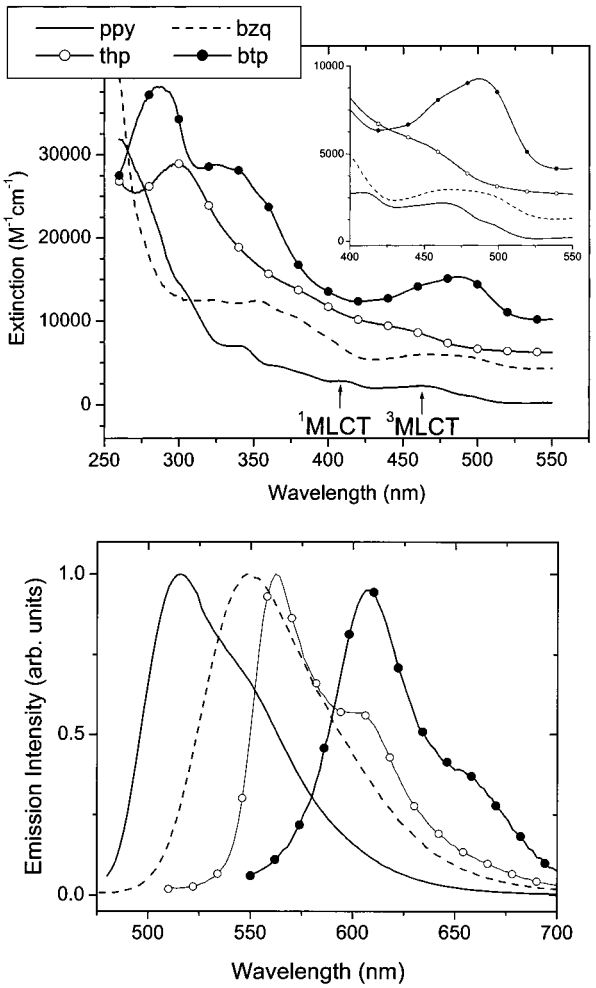

Figure 2. Absorption and luminescence spectra of $C^{\wedge}N_2$Ir(acac) complexes. (top) Absorption spectra for $C^{\wedge}N$ = *ppy*, *bzq*, *thp*, and *btp* complexes. The spectra have been offset for clarity. All four complexes have extinction coefficients of ~0.0 at 550 nm. (bottom) Photoluminescence spectra for the same complexes.

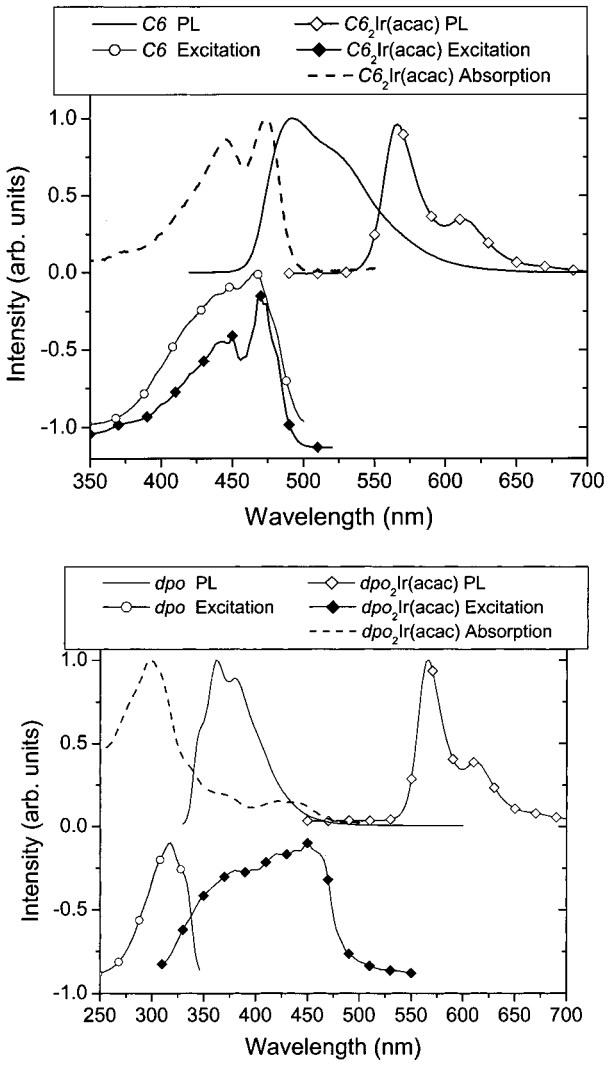

Figure 3. Solution photoluminescence, excitation, and absorption spectra of $C6_2$Ir(acac) and *C6* (top) and dpo_2Ir(acac) and *dpo* (bottom).

and $ppy_2Ir(\mu\text{-}Cl)_2Irppy_2$.[19] The *ppy*, *bzq*, *thp*, and *btp* complexes have very similar ^{3}MLCT energies, with λ_{max} values ranging from 440 to 490 nm (top inset of Figure 2 and Table 1). The similarity of MLCT energies for these complexes is not surprising, since all four complexes have MLCT states involving very similar (pyridyl) acceptors.

1. Correlation of Absorption and Emission Bands. In addition to ^{3}MLCT absorption bands with high oscillator strengths, strong spin−orbit coupling leads to efficient phosphorescence in the majority of the $C^{\wedge}N_2$Ir(LX) complexes reported here. The room-temperature (solution) quantum yields of these complexes range from 0.1 to 0.6 (Table 1), and their luminescent lifetimes fall between 1 and 14 μs, consistent with emission from a triplet excited state. The positions of the maximums in the excitation spectra for these complexes are very similar to those in their absorption spectra. Pumping either ligand-based or MLCT transitions efficiently gives the same phosphorescent excited state, as illustrated for $C6_2$Ir(acac) and dpo_2Ir(acac) in Figure 3.

Note that *C6* and *dpo* are common fluorescent laser dyes. Solutions of *C6* give green fluorescence, while solutions of *dpo* give UV/violet fluorescence.[20] Both of these laser dyes give high quantum efficiencies for fluorescence at room temperature and no observable phosphorescence. Further, *C6* and *dpo* have the requisite structures to make them suitable for cyclometalation reactions with Ir and have been used to make $C^{\wedge}N_2$Ir(acac) complexes. Coordination to Ir shifts the emission maximum of *C6* from 500 nm in the free dye to 570 nm for $C6_2$Ir(acac), as shown in Figure 3, providing striking evidence for intersystem crossing induced by the proximity of the heavy Ir atom. This Ir complex has a high quantum yield for emission of 0.6 and the lifetime is 14 μs. The excitation spectrum for $C6_2$Ir(acac) is very similar to that of pure *C6* and gives a good match to the absorption spectrum of the Ir complex. A more marked red shift is observed on metalation of *dpo*, whose λ_{max} for emission shifts from 365 nm for fluorescence from the free dye to 550 nm for phosphorescence from dpo_2Ir(acac). The excitation spectrum matches the absorption spectrum of dpo_2Ir(acac), with a maximum efficiency at an energy close to the MLCT band. The quantum efficiency and lifetime for the *dpo* Ir complex are 0.1 and 3 μs, as expected for Ir-promoted phosphorescence from the *dpo* ligand. The quantum yields for these phosphorescent transitions are high, especially $C6_2$Ir(acac), which has a quantum yield nearly as high as those of the fluorescent transition *C6* alone. In both *C6*- and *dpo*-based complexes, the Ir center facilitates intersystem crossing into the triplet levels of the laser

(19) Sprouse, S.; King, K. A.; Spellane, P. J.; Watts, R. J. *J. Am. Chem. Soc.* **1984**, *106*, 6647−6653.

(20) Brackman, U. *Lambdachrome Laser Dyes*, 2nd ed.; Lambda Physik Ink.: Göttingen, Germany, 1997.

dye and efficient phosphorescence from these low-energy triplet states. Efficient, ligand-based phosphorescence is common in *C^N*$_2$Ir(LX) complexes, making the design of new phosphors straightforward, as described below.

Although the *ppy*, *bzq*, *thp*, and *btp* complexes have similar MLCT absorption energies, their emission spectra differ markedly, Figure 2 (bottom). The *ppy* and *bzq* complexes exhibit a small Stokes shift between the ^{3}MLCT absorption and emission bands, while the *thp* and *btp* complexes give larger shifts. The energy differences between λ_{max} for the ^{3}MLCT absorption and emission spectra of *ppy*$_2$Ir(acac) and *bzq*$_2$Ir(acac) are 55 and 58 nm, respectively (~2200 cm^{-1}), wheras significantly larger shifts are observed for the *thp* and *btp* complexes (105 and 120 nm, respectively, ~4100 cm^{-1}). It has been shown that the emission spectra of *fac*-Ir*ppy*$_3$ and *fac*-Ir*thp*$_3$ complexes result from mixtures of MLCT and $^3(\pi-\pi^*)$ transitions.[21] *fac*-Ir*ppy*$_3$ emits from an excited state that is predominantly due to MLCT, while *fac*-Ir*thp*$_3$ emits from a largely ligand-based $^3(\pi-\pi^*)$ excited state. The $^3(\pi-\pi^*)$ level for phenylpyridine (*ppy*) has an energy of 460 nm,[22] which puts it at a sufficiently high energy such that the ^{3}MLCT becomes the lowest energy excited state. In contrast, the $^3(\pi-\pi^*)$ transition for thienylpyridine (*thp*) is at λ_{max} = 564 nm, which is at an energy below the ^{3}MLCT energy, so a predominantly ligand-based state is the lowest energy excited state in *fac*-Ir*thp*$_3$. The Stokes shifts observed for the *C^N*$_2$Ir(acac) complexes support similar assignments here. Emission from a predominantly ^{3}MLCT state would be expected to have a small Stokes shift between the ^{3}MLCT absorption and emission bands, as seen for *ppy* and *bzq* complexes. Emission from a predominantly ligand-based excited state, however, should give a large Stokes shift between the ^{3}MLCT absorption and emission bands, as observed for the *thp* and *btp* complexes.

The line shapes of the phosphorescence spectra of these complexes also support the hypothesis that the *ppy* and *bzq* complexes emit primarily from a MLCT state, while the other complexes emit from $^3(\pi-\pi^*)$ *C^N* states. The emission spectra for *thp*$_2$Ir(acac) closely resemble the phosphorescence spectrum reported for the free organic ligand,[7,17,23] supporting the assignment of the lowest energy excited state to be predominantly ligand-based.[24] Vibronic fine structure is clearly observed for the *thp* and *btp* ligands and is absent for the *ppy* and *bzq* complexes. Emission bands from MLCT states are generally broad and featureless, while $^3(\pi-\pi^*)$ states typically give highly structured emission.[25] Significant vibronic fine structure is also observed in the PL spectra of both the *C6* and *dpo* complexes, consistent with emission from ligand-based excited states in these complexes as well.

2. C^N Ligand Tuning of Phosphorescence. Further evidence for significant ligand character in the emission spectra can be seen in a series of *C^N*$_2$Ir(acac) complexes prepared with *bo*, *bt*, *bon*, and α*bsn* ligands. The photoluminescence spectra of these complexes show a pronounced red shift, Figure 4.

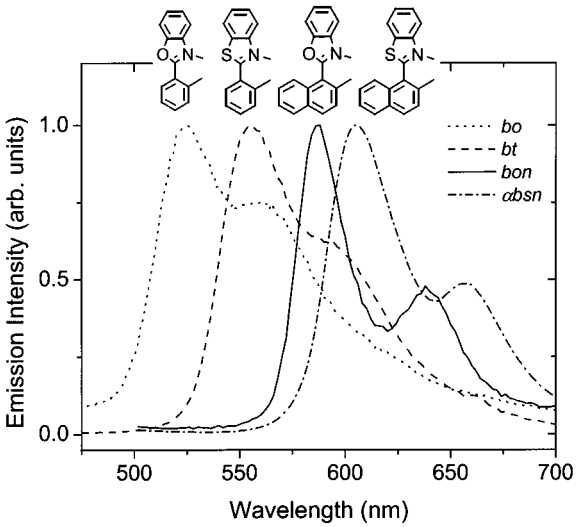

Figure 4. Solution photoluminesccence spectra of *bo*$_2$Ir(acac), *bt*$_2$Ir(acac), *bon*$_2$Ir(acac) and α*bsn*$_2$Ir(acac). The structures of the individual *C^N* ligands are shown above the corresponding spectrum.

All four complexes show vibronic fine structure in their emission spectra, as expected for ligand-based transitions. The highest energy emission is observed for the benzoxazole (*bo*) complex. Substitution of S for O in a chromophore (*bo* → *bt*) leads to a 30-nm red shift, due the higher polarizibility and basicity of sulfur relative to oxygen,[26] in this ligand-based excited state. Increasing the size of the ligand π system is expected to bathochromically shift electronic transitions, as is observed in converting a phenyl group to a naphthyl group (*bo* → *bon*), which leads to a 60-nm red shift. The effects of the naphthyl and sulfur substitutions are nearly additive, leading to an 80-nm red shift when comparing *bo* to α*bsn* complexes. Unfortunately, we have been unable to detect phosphorescence spectra from the free ligands, even at temperatures below 10 K, so we cannot directly correlate the phosphorescence spectra of the Ir complexes with those of the $^3(\pi-\pi^*)$ of the free ligands. The luminescence energies of the four Ir complexes do follow the same trend seen in the fluorescence spectra of the free ligands, however, which have λ_{max} values of 350, 360, 380 and 400 nm, respectively.

We also attempted to decrease the size of the ligand π system, in the hope of achieving a shift form green to blue emission. The first approach we chose was to replace the metalated phenyl group of the *ppy* ligand with a smaller group, such as a vinyl or cycloalkene (e.g., *C^N* = 2-vinylpyridine, vinylbenzoxazole, and 1-cyclohexenylbenzoxazole). Unfortunately, we have been unable to cyclometalate ligands in which the phenyl has been replaced with olefinic groups. We have succeeded in decreasing the size of the π system in the benzoxazole portion of the ligand, however, i.e., *op* (2-(1-phenyl)oxazole, Figure 1). In *op*, the phenylene group of the *bo* benzoxazole group has been replaced with a vinylene group. The emission spectrum of *op*$_2$Ir(acac) has its λ_{max} at 520 nm, only 5-nm blue shifted from *bo*$_2$Ir(acac), Table 1. The π^* state in both of these complexes is presumably localized in the oxazole group and does not extend significantly into the added phenyl ring of the benzoxazole group, leading to only a modest shift in the phosphorescence energy on removal of the phenyl ring.

Two different isomers of the naphthylbenzothiazole (α*bsn* and β*bsn*) have been used to prepare cyclometalated Ir

(21) (a) Colombo, M. G.; Brunold, T. C.; Riedener, T.; Güdel, H. U.; Förtsch, M.; Bürgi, H.-B. *Inorg. Chem.* **1994**, *33*, 545−550. (b) Colombo, M. G.; Hauser, A.; Gudel, H. U. *Inorg. Chem.* **1993**, *32*, 3088−3092.

(22) Sarkar, A.; Sankar, C. *J. Lumin.* **1995**, *65*, 163−168.

(23) Colombo, M. G.; Hauser, A.; Güdel, H. U. *Top. Curr. Chem.* **1994**, *171*, 143−171 (Electronic and Vibronic Spectra of Transition Metal Complexes I).

(24) Sandrini, D.; Maestri, M., Ciano, M.; Balzani, V.; Lueoend, R.; Deuschel-Cornioley, C.; Chassot, L.; von Zelewsky, A. *Gaz. Chim. Ital.* **1988**, *118*, 661.

(25) Sandrini, D.; Maestri, M., Ciano, M.; Balzani, V.; Deuschel-Cornioley, C.; von Zelewsky, A.; Jolliet, P. *Helv. Chim. Acta* **1988**, *71*, 1053. Balton, C. B.; Murtaza, Z.; Shaver, R. J.; Rillema, D. P. *Inorg. Chem.* **1992**, *31*, 3230.

(26) Zollinger, H. *Color Chemistry: Syntheses, Properties and Applications of Organic Dyes and Pigments*, 2nd ed.; VSH: Weinheim, Germany, 1991.

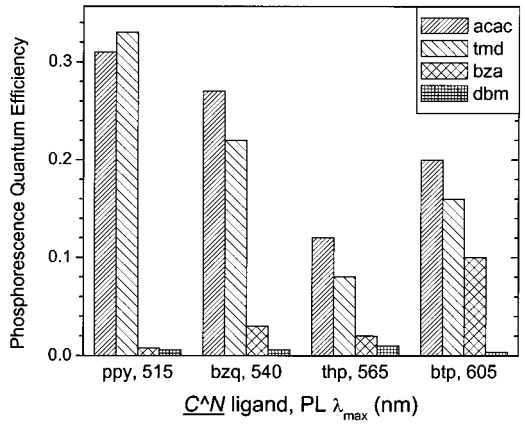

Figure 5. Solution phosphorescence efficiencies of C^N_2Ir(LX) as a function of the LX ligand for acac, tmb, bza, and dbm (see Figure 1).

complexes. The only chemical difference between these complexes is the substitution at the naphthyl groups. The emission efficiencies, lifetimes, and emission spectral line shapes of the two complexes are similar. The principal difference in the photophysical properties of α*bsn* and *β*bsn complexes are blue shifts in the phosphorescence and absorption spectra of the *β*bsn relative to the α*bsn* complex (e.g., emission $\lambda_{max} = 593$ and 606 nm, respectively). Both phosphorescence spectra show vibronic fine structure, consistent with ligand-based emission. Unfortunately, we have been unable to observe phosphorescence from frozen solutions of the α*bsn* and *β*bsn free ligands, so we cannot determine if the blue shift for the *β*-isomer is due the electronic structure of the two ligands. On the basis of the photophysics of related naphthyl complexes, the *β*bsn blue shift is most likely not related to the Ir substitution. Similar blue shifts are observed in other acceptor substituted naphthalene derivatives, substituted in the 1 (α)- and 2 (*β*)-positions. For example, the phosphorescence energy of 2-nitronaphthalene is blue shifted relative to that of 1-nitronaphthalene by 16 nm.[27]

3. C^N vs LX Centered Emission. Three *fac*-IrC^N_3 complexes have been reported, i.e., *fac*-Ir(*ppy*)$_3$,[28] *fac*-Ir(*bzq*)$_3$,[9] and *fac*-Ir(*thp*)$_3$.[29] All three tris-chelate complexes have emission spectra that are nearly identical to the C^N_2Ir(acac) complexes with the same ligands.[9] The phosphorescence quantum yields and lifetimes for the two classes of complex for a given ligand are also the same. The similarity of the two classes of complexes is consistent with emission predominantly from the "C^N_2Ir" fragment in C^N_2Ir(acac) complexes.

For all of the complexes discussed thus far, the triplet levels of the LX ligand (acac) lie well above the energies of the *C^N* ligand and MLCT excited states. Thus, the luminescence is dominated by *C^N* and MLCT transitions, leading to efficient phosphorescence. If the triplet-state energy of the LX ligand is lower in energy than the *C^N* $^3(\pi-\pi^*)$ or ^{3}MLCT, however, a triplet LX level will be the lowest energy excited state. A switch from "C^N_2Ir" to LX-based emission can be seen in a series of complexes prepared with different *β*-diketonates (i.e., acac, tmd, bza, and dbm in Figure 1). The phosphorescence quantum efficiencies for these complexes are provided in the bar graph of Figure 5. The emission spectra and phosphorescence efficiencies for the tmd complexes of *ppy*, *bzq*, *thp*, and *btp* are identical to those of the same complexes prepared with an acac LX ligand. All of these complexes emit from states within the "C^N_2Ir" fragment as discussed above. When the LX ligand is bza, emission from the *ppy*, *bzq*, and *thp* complexes are largely quenched ($\phi_{phos} < 0.01$). In contrast, the *btp* complex (*btp*$_2$Ir(bza)) gives a quantum efficiency of 0.1 and an emission spectrum identical to that of *btp*$_2$Ir(acac). For the C^N_2Ir(dbm) complexes, all four *C^N* ligands give very weak phosphorescence ($\phi_{phos} < 0.01$). The triplet levels of these three *β*-diketonates fall in the order tmd > bza > dbm. Apparently, only the ligand with the lowest triplet energy, i.e., *C^N* = *btp*, has a triplet level lower than dbm. Thus, only the *btp* complex gives emission from an excited state on the "C^N_2Ir" fragment for bza complexes. The other three complexes have their excited states localized predominantly on the on the bza ligand, leading to weak phosphorescence. All four *C^N* ligands give "(C^N)$_2$Ir" fragments with triplet levels higher than dbm, so the emission results from a dbm-based excited state, giving rise to very inefficient phosphorescence for all four *C^N* ligands.

4. OLEDs Prepared with C^N_2Ir(LX) Complexes. Using the phosphors discussed above it is possible to prepare efficient OLEDs, which emit in a variety of colors. The OLED structure used is the same one previously developed for *fac*-Ir(*ppy*)$_3$-based OLEDs, which gave green electroluminescence (EL), at an external efficiency of 9% (η_{ext}, photons/electrons).[30] In the C^N_2Ir(acac)-based devices, the Ir phosphor was doped into the emissive layer of the OLED, at a concentraion of 7 wt %. Figure 6 (top) shows external quantum efficiency (η_{ext}) and power efficiency as functions of current density for OLEDs with a *ppy*$_2$Ir(acac) dopant. A maximum external quantum efficiency (η_{ext}) of 12.3 ± 0.3% and a power efficiency of 38 ± 3 lm/W[31] were obtained at a current density 0.01 mA/cm^2. The device showed a gradual decrease in η_{ext} with increasing current density, which is attributed to increasing triplet−triplet annihilation of the phosphor-bound excitons.[10−12] A maximum optical output of 32 500 cd/m^2 was obtained at $J = 2.4$ A/cm^2.

OLEDs prepared with *btp*$_2$Ir(acac) gave a peak quantum efficiency of 6.6% and a power efficiency of 2.2 lm/W (at 1 mA/cm^2). The external quantum efficiency and power efficiency as functions of current density for *btp*$_2$Ir(acac) based OLEDs are shown in Figure 6 (bottom). These efficiency values are the highest values reported for a red emissive OLED. Table 2 summarizes the EL performance with *ppy*$_2$Ir(acac), *bt*$_2$Ir(acac), and *btp*$_2$Ir(acac) doped OLEDs. These devices give high performance with EL emission colors in green, yellow, and red, respectively. The device structures and layer thickness used here were identical to those reported for *fac*-Ir(*ppy*)$_3$-based OLEDs.[10(b)] They have not been optimized for either low-voltage or high-efficiency operation, so the quantum and power efficiency values are lower limits. For example, lowering the doping concentration of *bt*$_2$Ir(acac) from 7 to 4% increases the maximum η_{ext} from 9.5 to 11.9%, Figure 6 (middle). Data are also shown for an OLED in which the *bt*$_2$Ir(acac)-doped CBP film has been replaced with a pure *bt*$_2$Ir(acac) luminescent film. Increasing the concentration of *bt*$_2$Ir(acac) to 100% lowers the device efficiency to 1.5%, due to enhanced self-quenching in the neat *bt*$_2$Ir(acac) film. The device performances and electrical properties of the three C^N_2Ir(LX)-based OLEDs are very similar, which is consistent with similar mechanisms for exciton formation and trapping at the phosphorescent centers. The lower

(27) Rusakowicz, R.; Testa, A. C. *Spectochim. Acta, Part A* **1971**, *27*, 787−92.

(28) (a) Garces, F. O.; King, K. A.; Watts, R. J. *Inorg. Chem.* **1988**, *27*, 3464−3471. (b) Dedian, K.; Djurovich, P. I.; Garces, F. O.; Carlson, G.; Watts, R. J. *Inorg. Chem.* **1991**, *30*, 1685−1687.

(29) Colombo, M. G.; Brunold, T. C.; Riedener, T.; Güdel, H. U.; Förtsch, M.; Bürgi, H.-B. *Inorg. Chem.* **1994**, *33*, 545−550.

(30) Baldo, M. A.; Lamansky, S.; Burrows, P. E.; Thompson, M. E.; Forrest, S. R. *Appl. Phys. Lett.* **1999**, *75*, 4−6.

(31) The lumen is a unit of optical power that is weighted by the human eye response. For the EL spectrum of *ppy*$_2$Ir(acac), there are roughly 500 lumens/optical watt.

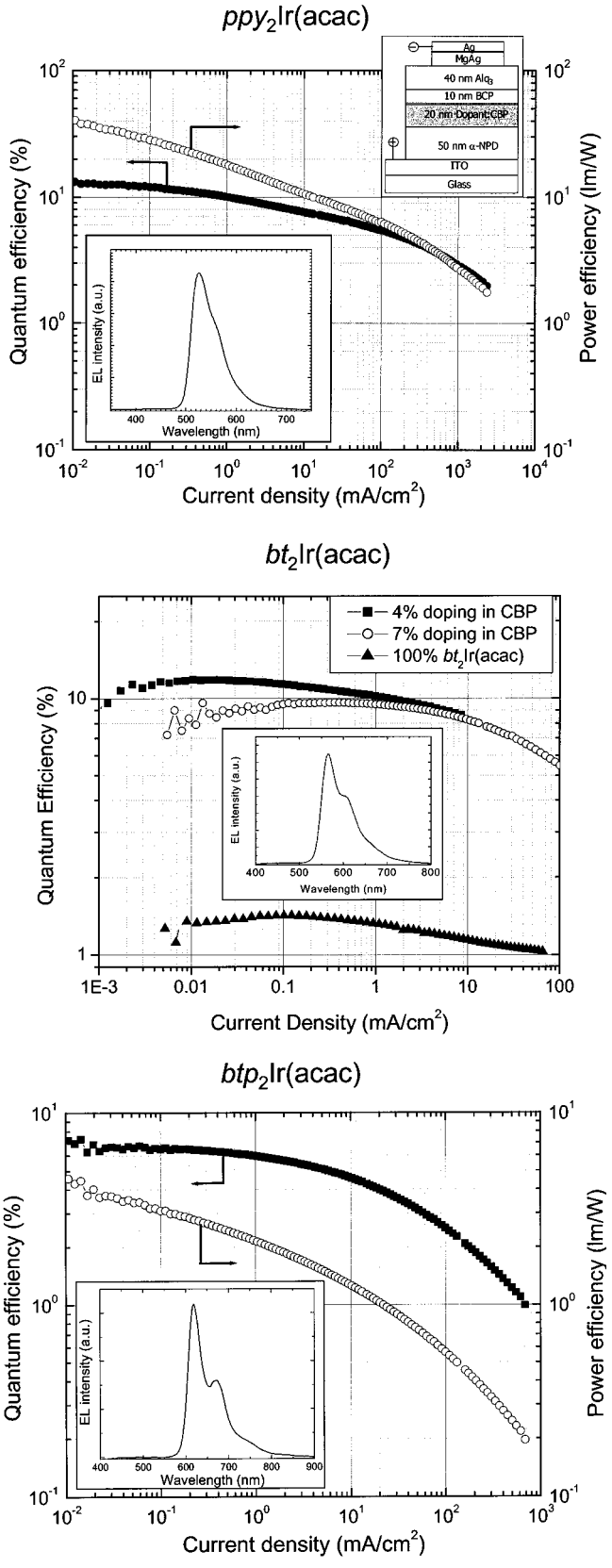

Figure 6. External quantum and power efficiencies of OLEDs using ppy_2Ir(acac):CBP (top), bt_2Ir(acac):CBP and bt_2Ir(acac) (middle), and btp_2Ir(acac):CBP (bottom) emissive layers. The inset to the top plot shows the OLED structure used in this study. The EL spectrum of each device is shown as an inset on the relevant plots. α-NPD = 4,4′-bis-[*N*-(naphthyl-*N*-phenylamino)biphenyl, CBP = 4,4′-*N*,*N*′-dicarbazolyl-biphenyl, BCP = 2,9-dimethyl-4,7- diphenyl-1,10-phenanthroline (bathocuproine), and Alq_3 = tris(8-hydroxyquinoline)aluminum.

Table 2. OLED Performance of ppy_2Ir(acac)-, bt_2Ir(acac)-, and btp_2Ir(acac)-Based OLEDs[a]

	dopant phosphor		
	ppy_2Ir(acac)	bt_2Ir(acac)	btp_2Ir(acac)
EL color	green	yellow	red
peak wavelength (nm)	525	565	617
CIE-x	0.31	0.51	0.68
CIE-y	0.64	0.49	0.33
luminance at 10 mA/cm^2(cd/m^2)	3.300	2500	470
drive voltage (V) at 10 mA/cm^2	9.3	9.5	11.6
ext quantum effic (%)			
at 1 mA/cm^2	10.0	9.7	6.6
at 10 mA/cm^2	7.6	8.3	6.0
at 100 mA/cm^2	5.4	5.5	4.6
power effic (lm/W) at 1 mA/cm^2	18	11	2.2

[a] Device structure, ITO/α-NPD (500 Å)/doped CBP (300 Å)/BCP (100 Å)/Alq_3 (400 Å)/Mg−Ag. All three devices were prepared with the dopant at a 7% loading in the CBP layer.

efficiency of the *btp* $_2$Ir(acac)-based OLED relative to the ppy_2-Ir(acac) and bt_2Ir(acac) may be due to a lower phosphorescence efficiency of the *btp* complex relative to the *ppy* and *bt* complexes.

The EL spectra of the $C\hat{}N_2$Ir(acac)-based devices match those of the same phosphors in a dilute solution. Thus, all EL emission originates from the triplet excited states of the phosphors. The Commission Internationale de L'Eclairage (CIE) coordinates for the three OLEDs are shown in Figure 7 (left). The CIE system is the standard for evaluating color quality for visual applications.[32] The btp_2Ir(acac)-doped OLED gives a saturated red emission that has CIE coordinates close to the National Television Standards Committee (NTSC) recommended red for a cathode ray tube (CRT). Green emission from ppy_2Ir(acac) is very similar to Ir(ppy)$_3$-based OLEDs and a common fluorescence-based green OLED (Coumarin6:Alq_3). The three complexes used to fabricate OLEDs were chosen to be representative of the family of $C\hat{}N_2$Ir(LX) phosphors. Figure 7 (right) shows the CIE coordinates of the solution phosphorescent spectra of all of the $C\hat{}N_2$Ir(acac) complexes reported here. All of the $C\hat{}N_2$-Ir(acac) complexes are expected to give OLEDs with efficiencies similar to those reported for the *ppy*, *bt*, and *btp* complexes. We expect that the EL and photoluminescence spectra of these phosphors are similar, so the coordinates of the phosphorescence spectra shown in Figure 7 (right) will likely be the same for OLEDs prepared with these phosphors. The $C\hat{}N_2$Ir(acac) are clearly a broad and widely tunable class of OLED phosphors.

Summary

It has been reported that phosphorescence in iridium tris-cyclometalated complexes comes from a mixture of ligand centered, $^3(\pi-\pi^*)$, and ^{3}MLCT excited states.[7,33] While phosphorescence results from a mixture of the two triplet states (and the ^{1}MLCT via spin−orbit coupling), the emissive excited state is predominantly $^3(\pi-\pi)$ or ^{3}MLCT, depending on the energies of the two excited states. The same situation is present in the $C\hat{}N_2$Ir(LX) complexes. ppy_2Ir(acac), tpy_2Ir(acac), and bzq_2Ir-(acac) have high-energy $^3(\pi-\pi)^*$ states and, thus, give unstructured, predominantly ^{3}MLCT emission. The other complexes reported here give phosphorescence spectra with a reasonable

(32) Whitaker, J., *Electronic Displays: Techlnology, Design, and Applications;* McGraw-Hill: New York, 1994; p 92.
(33) Colombo, M. G.; Hauser, A.; Gudel, H. U. *Inorg. Chem.* **1993**, *32*, 3088−3092.

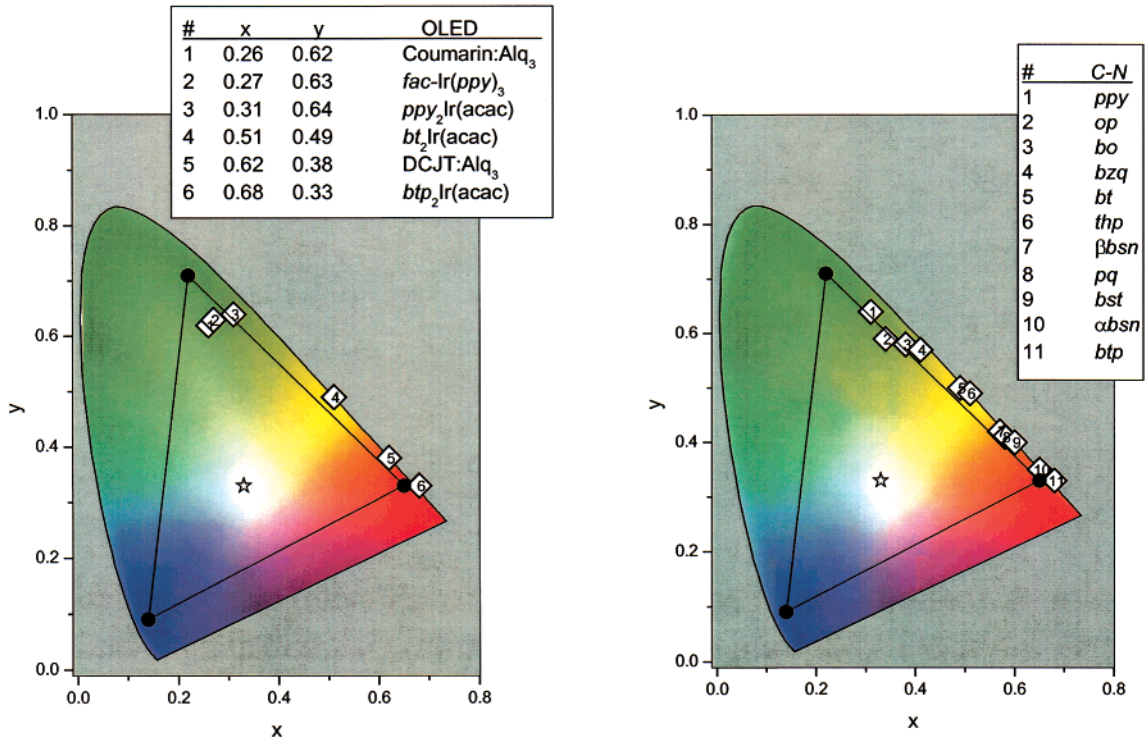

Figure 7. The Commission Internationale de L′Eclairage (CIE) chromaticity coordinates of OLEDs and phosphorescence spectra of $C\hat{}N_2$Ir(LX) complexes. The CIE coordinates for OLEDs with ppy_2Ir(acac):CBP, bt_2Ir(acac):CBP, and btp_2Ir(acac)Ir:CBP are shown relative to the fluorescence-based devices, coumarine6:Alq_3 and DCJT:Alq_3 on the left. The CIE coordinates of the phosphorescence spectra of many of the $C\hat{}N_2$Ir(LX) complexes prepared here are shown to the right. The NTSC standard coordinates for the red, green, and blue subpixels of a CRT are at the corners of the black triangle.

degree of vibronic fine structure and significant Stokes shifts, consistent with predominantly $^3(\pi-\pi)^*$ $C\hat{}N$-based emission. By changing the $C\hat{}N$ ligands in cyclometalated Ir complexes, we demonstrated green to red electrophosphorescence with high η_{ext}. High phosphorescence efficiencies and lifetimes less than 10 μs resulted in record high-performance OLEDs operating from the green to the red. We note that the device structure has the potential for further optimization. For example, the use of Li-based cathodes,[12,34] optimization of dopant concentration and thickness of organic layers, and other device configurations[11] can result in a reduction of operating voltage and increased quantum efficiency.

Acknowledgment. The authors thank Universal Display Corp., the Defense Advanced Research Projects Agency, and the National Science Foundation for financial support of this work.

Supporting Information Available: Synthetic and spectroscopic data for all of the $C\hat{}N_2$Ir(LX) complexes where LX = tmd, bza, and dbm reported in this paper. This material is available free of charge via the Internet at http://pubs.acs.org.

JA003693S

(34) Hung, L. S.; Tang, C. W.; Mason, M. G. *Appl. Phys. Lett.* **1997**, *70*, 152.